# Adaptive PI Controller for Slip controlled Belt Continuously Variable Transmission

**Florian Verbelen** [*,***] **Michiel Haemers** [*,**,***]
**Jasper De Viaene** [*,**] **Stijn Derammelaere** [**,***]
**Kurt Stockman** [*,***] **Peter Sergeant** [*,***]

[*] *Department of Electrical Energy, Metals, Mechanical Constructions and Systems, Ghent University, Belgium (e-mail: florian.verbelen@ugent.be).*
[**] *Department of Electromechanics, Op3Mech, University of Antwerp, Belgium*
[***] *Member of EEDT partner of Flanders Make, www.eedt.ugent.be*

**Abstract:** The control of slip in a belt Continuously Variable Transmission (CVT) has been the subject of many research papers. Optimal control of the belt CVT is of major importance for the efficiency as demonstrated in literature. The challenge in optimizing that efficiency is in the reduction of the necessary clamping forces while the stability of the variable transmission is maintained. Although these problems have already been tackled to a certain extent, mostly fairly complex controllers are proposed. The goal of this paper is to propose a straightforward though effective method to control slip. The main idea of the paper is to use linearized equations of the slip dynamics to update the controller parameters in function of the operating point. This approach allows to reduce the highly nonlinear system to a first order transfer function which is easily controlled with a PI controller. Results based on extensive simulations show that the controller is robust against torque disturbances and speed ratio variations.

*Keywords:* Adaptive control, PI controllers, mechanical systems, dynamic models

## 1. INTRODUCTION

Manufacturers of advanced drive trains specialized in the automotive industry encounter an ever growing pressure due to increasingly stringent regulation concerning fuel consumption and emissions. As a result, they are forced to innovate and one of those innovations is the Continuously Variable Transmission (CVT). In a CVT the speed ratio can be varied continuously between two finite values.

Many types of CVT are discussed in literature, e.g. toroidal CVT (Carbone et al. (2004)), belt CVT (Carbone et al. (2007)), Milner CVT (Akehurst et al. (2007)), hydraulic CVT (Kempermann (2007)), wheel type CVT (Chen et al. (2017)), ... However, the belt CVT is the most commonly used CVT, among all, in automotive applications (Srivastava and Haque (2009)).

The ratio variation abilities of the belt CVT are used in a vehicle to enable the Internal Combustion Engine (ICE) to operate in its most optimal operating point, which results in lower fuel consumption as demonstrated by Carbone et al. (2001) and Van der Sluis et al. (2006). Despite the potential of the technology, a significant part of the fuel savings is lost due to the low efficiency of the variable transmission.

The main reason for the CVTs low efficiency are the high clamping forces which are used to transfer torque. These clamping forces, delivered by hydraulic cylinders, are typically chosen 30% too high to ensure stable operation by preventing gross slip at all times (Bonsen et al. (2005b)). This urge for stability will increase the losses in the hydraulic circuit significantly. Another negative side-effect of this control strategy is increased wear and thus reduced life span of the transmission.

The efficiency can be increased by lowering the clamping forces but than a robust slip controller is necessary. Bonsen et al. (2005b) elaborated such a controller based on the slip dynamics of the CVT and the PID design methodology described by Panagopoulos et al. (2002). The results show a substantial increase in the efficiency of the drive train while slip is still adequately controlled.

The objective of this paper is to demonstrate that the highly non linear slip dynamics can be reduced to a first order system. Therefore no complex control design rules, as used in Bonsen et al. (2005b), are necessary.

This paper is structured as follows. Section 2 shortly discusses the operating principle of the belt CVT. Thereafter the slip dynamics are derived and linearized in section 3. Section 4 discusses the design and implementation of the controllers while the results are presented in section 5. Finally, in Section 6 the conclusions of the research are formulated.

## 2. OPERATING PRINCIPLE

The belt CVT consists of 2 pulleys which are composed of a fixed half and a movable half (sheave), see Fig. 1. By adapting the position of the movable sheaves, the belt

 

runs on another radius and as a result the speed ratio $\tau_s$ is altered. Movement of the sheaves and thus control of the speed ratio is done via 2 hydraulic cylinders which deliver a force on the primary $F_p$ and secondary $F_s$ pulley. Consequently the belt CVT is a Multiple Input Multiple Output (MIMO) system: the forces (input) will not only be used to control the speed ratio (output) but also to control the slip (output) as mentioned in the introduction. Moreover the clamping force on the secondary pulley is used for slip control purposes while the ratio of both clamping forces is used to control the speed ratio as demonstrated by Carbone et al. (2007).

## 3. LINEARIZED SLIP DYNAMICS

As demonstrated by Bonsen et al. (2005b), it is vital to model the slip dynamics in order to design a proper slip controller. The model is based on Fig. 1 in which $T_{ICE}$ and $T_{load}$ are respectively the engine torque and load torque, the inertia of both pulleys is denoted by $J_p$ and $J_s$ and the speed by $\omega_p$ and $\omega_s$. Subscript $p$ stands for the primary side while subscript $s$ stands for the secondary side.

Besides engine $T_{ICE}$ and load torque $T_{load}$, $T_p$ and $T_s$ are mentioned on Fig. 1. These variables represent the torque produced via friction and are calculated as follows (Bonsen et al. (2005b)):

$$T_{p,s} = \frac{2F_s\mu\left(\nu\right)R_{p,s}}{\cos\beta} \tag{1}$$

with $\beta$ the half cone angle of the pulleys, $\mu$ the friction coefficient which depends on $\nu$ the slip and $R_{p,s}$ the running radii of the belt.

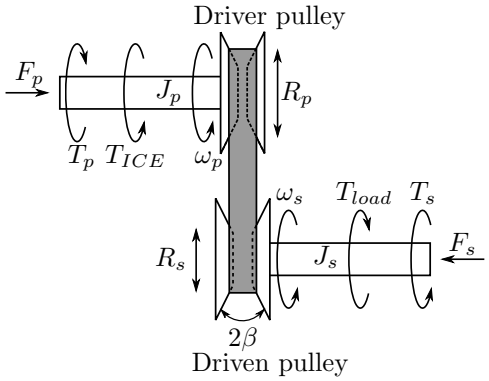


Fig. 1. Belt CVT

When the speed ratio is varied or there is any load disturbance or variation, slip variations will occur. Slip $\nu$ is defined by the ratio of the actual speed ratio $\tau_s$ and the theoretical or geometrical speed ratio $\tau_t$, see eq. (2). In eq. (2), the actual speed ratio $\tau_s$ is calculated as the ratio of the secondary $\omega_s$ and primary speed $\omega_p$ while the theoretical speed ratio $\tau_t$ is defined by the ratio of the primary $R_p$ and secondary radius $R_s$.

$$\nu = \frac{-\tau_s}{\tau_t} + 1 = \frac{\frac{\omega_s}{\omega_p}}{\frac{R_p}{R_s}} + 1 \tag{2}$$

As it is the objective to control the variations in slip, the derivative is considered:

$$\dot{\nu} = \frac{\dot{\tau}_t\tau_s - \dot{\tau}_s\tau_t}{\tau_t^2} \tag{3}$$

Which can be rewritten as:

$$\dot{\nu} = \frac{\dot{\tau}_t\frac{\omega_s}{\omega_p} - \frac{\dot{\omega}_s\omega_p - \dot{\omega}_p\omega_s}{\omega_p^2}\tau_t}{\tau_t^2} \tag{4}$$

The derivatives of the primary $\dot{\omega}_p$ and secondary speed $\dot{\omega}_s$ in eq. (4) can be replaced by respectively eq. (5) and eq. (6).

$$\dot{\omega_p} = \frac{T_{ICE} - T_p}{J_p} \tag{5}$$

$$\dot{\omega_s} = \frac{T_s - T_{load}}{J_s} \tag{6}$$

Considering eq. (5) and (6), eq. (4) can be redrafted in terms of torque and inertia:

$$\dot{\nu} = \frac{\dot{\tau}_t\omega_s}{\tau_t^2\omega_p} - \frac{T_s - T_{load}}{\omega_p J_s\tau_t} + \frac{\left(T_{ICE} - T_p\right)\left(1-\nu\right)}{\omega_p J_p} \tag{7}$$

By using eq. (1), the equation describing the slip dynamics can be finalized:

$$\begin{aligned}\dot{\nu} = \frac{\dot{\tau}_t\omega_s}{\tau_t^2\omega_p} + \frac{1}{\omega_p}\left(-\frac{2F_s\mu R_s}{J_s\cos\beta\tau_t} + \frac{T_{load}}{J_s\tau_t}\right) \\ + \frac{1-\nu}{\omega_p}\left(-\frac{2F_s\mu R_s\tau_t}{J_p\cos\beta} + \frac{T_{ICE}}{J_p}\right)\end{aligned} \tag{8}$$

The variation in slip is thus a function of 10 variables:

$$\dot{\nu} = f\left(\nu, \dot{\tau}_t, \tau_t, \omega_s, \omega_p, F_s, R_s, T_{ICE}, T_{load}, \mu\right) \tag{9}$$

Of these variables, only the secondary clamping force $F_s$ can be used to actively control the slip. All other variables are controlled at a higher level by for example the energy management system which selects optimal operating points ($T_{ICE}$, $\omega_p$, ...) or are induced by the considered load profile ($T_{load}$, $\omega_s$, ...). Therefore, these variables are considered as disturbances $D$.

Notice that the primary clamping force $F_p$ does not appear in the equation. However, this does not mean that $F_p$ has no impact on the slip. As shortly mentioned in section 2, the speed ratio $\tau_t$ of the CVT depends on the ratio of the clamping forces. Consequently, an increase of $F_p$ will lead to a variation in speed ratio $\tau_t$. As the speed ratio has an impact on the slip dynamics (see eq. (8)), $F_s$ will also have to change to maintain the desired slip value. The secondary clamping force has thus an indirect effect on the slip.

In the following paragraphs, the slip dynamics are linearized for control purposes. However, the model of the CVT which is used to test the behavior of the elaborated controller, is not simplified to any extend. If eq. (8) is linearized, ignoring the variables considered as disturbances $D$, the following equation is found:

$$\begin{aligned}\dot{\nu} = D_{\dot{\tau}_t} + D_{\tau_t} + D_{\omega_s} + D_{\omega_p} + \left.\frac{\partial f}{\partial F_s}\right|_* \left(F_s - F_s^*\right) + D_{R_s} \\ + D_{T_{load}} + D_{T_{ICE}} + \left.\frac{\partial f}{\partial \nu}\right|_* \left(\nu - \nu^*\right) + D_\mu\end{aligned} \tag{10}$$

$$\dot{\nu} = D + \left.\frac{\partial f}{\partial F_s}\right|_* \left(F_s - F_s^*\right) + N_{R_s} + \left.\frac{\partial f}{\partial \nu}\right|_* \left(\nu - \nu^*\right) \tag{11}$$

Which can be rewritten as:

$$\dot{\nu} = D \underbrace{- \left.\frac{\partial f}{\partial F_s}\right|_* F_s^* - \left.\frac{\partial f}{\partial \nu}\right|_* \nu^*}_{\text{K}} + \underbrace{\left.\frac{\partial f}{\partial F_s}\right|_*}_{\text{L}} F_s + \underbrace{\left.\frac{\partial f}{\partial \nu}\right|_*}_{\text{M}} \nu \tag{12}$$

In which the partial derivative of $F_s$ equals:

$$\frac{\partial f}{\partial F_s}\Big|_* = -\frac{2\mu R_s}{\omega_p J_s \cos\beta \tau_t} - \frac{(1-\nu)\,2\mu R_s \tau_t}{\omega_p J_p \cos\beta} = L \tag{13}$$

And the partial derivative of $\nu$:

$$\frac{\partial f}{\partial \nu}\Big|_* = \frac{2F_s \mu R_s \tau_t}{\omega_p J_p \cos\beta} - \frac{T_{ICE}}{\omega_p J_p} = M \tag{14}$$

The next step is to take the Laplace of eq. (12):

$$\nu(s)s = K + LF_s(s) + M\nu(s) \tag{15}$$

Note that the disturbance term has been removed as it has no impact on the actual linearized transfer function. The term $K$ can also be removed as it is merely an offset which can be ignored for control purposes. Therefore, the following transfer function is found:

$$\frac{\nu(s)}{F_s(s)} = \frac{\frac{-L}{M}}{\frac{-1}{M}s + 1} \tag{16}$$

This means that the complex nonlinear behavior of the slip dynamics is now converted to a first order system which can be easily controlled.

## 4. CONTROLLER DESIGN AND IMPLEMENTATION

### *4.1 Control architecture*

The belt CVT is a MIMO system as highlighted in section 2. To decouple the control loop of the ratio and the slip the scheme presented in Fig. 2 is used. In this scheme, the ratio controller yields the ratio of the forces on the primary and secondary pulley while the slip controller yields the force on the secondary pulley.

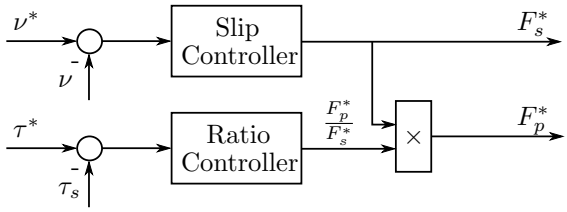


Fig. 2. Control architecture

### *4.2 Ratio controller*

As control algorithm, a PI controller is chosen, which has been tuned based on the work of Simons et al. (2008). A differential action is not necessary as the shifting process exhibits a sufficient amount of damping (Simons et al. (2008)). The implementation of this PI controller with fixed $K_p$ and $T_i$ is rather trivial and is therefore not further discussed.

### *4.3 Slip controller*

Based on section 3 it is known that the slip dynamics can be described as a first order system. Therefore a PI controller should result in acceptable slip behavior. The transfer function of a PI controller can be written as:

$$TF_{PI} = K_p\left(\frac{T_i s + 1}{T_i s}\right) \tag{17}$$

with the proportional term $K_p$ and the integral term $T_i$. The integral term should be equal to the time constant of the first order system depicted by eq. (16). If the system pole is canceled by the controller zero, the dynamical behavior can be uniquely defined by the control parameter $K_p$. $T_i$ is therefore equal to:

$$T_i = \frac{-1}{M} \tag{18}$$

Note that this can only be done if the pole is in the left half plane (see Fig. 3 a)) which means that $M$ needs to be negative. This will be the case if $T_{ICE} > T_s\tau_t$ which is valid for almost all operating conditions. Only when the ICE is turned off while the belt is still rotating this method becomes erroneous. However this is an unlikely event as the ICE is only turned off when the vehicle is close to a standstill or is at standstill. In that case, slip control is no longer necessary. To calculate the proportional term, the closed loop system is taken into account:

$$TF_{CL} = \frac{\frac{-L}{M}K_p}{T_i s + \frac{-L}{M}K_p} \tag{19}$$

Which means that the closed loop pole defining the closed loop dynamics can be found at:

$$s = \frac{\frac{L}{M}K_p}{T_i} \tag{20}$$

By which the proportional gain of the controller can be defined with one degree of freedom $\alpha$:

$$K_p = \frac{\alpha T_i}{\frac{L}{M}} = \frac{-\alpha}{L} \tag{21}$$

The value $\alpha$ defines the position of the closed loop pool as demonstrated in Fig. 3 (red line) and is related to the ability to handle disturbances as will be demonstrated in section 5. The black cross resembles the system pole while the blue cross and circle resemble respectively the pole and zero of the PI controller. Only case a) is discussed in this paper because of the previously mentioned reason.

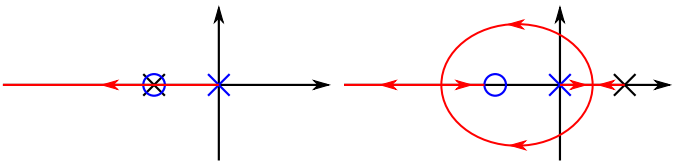

a) b)

Fig. 3. a) Root locus for the case in which $T_{ICE} > T_s\tau_t$: left half plane system pole. b) Root locus for the case in which $T_{ICE} < T_s\tau_t$: right half plane system pole.

The implementation of the PI controller comes thus down to the determination of parameters $L$ and $M$. Parameter $L$ is calculated based on eq. (13) while parameter $M$ can be determined with eq. (15).

The many parameters in those equations define the operating point based on which the linearization is done. As all inputs of eq. (13) and eq. (15) are constantly varying, the equations need to be solved repeatedly during simulation

to feed the PI controller with the optimal $K_p$ and $T_i$ at all times. However, the computational effort of solving these static relations is negligible.

Another complexity of the determination of $L$ and $M$ is the number of parameters which need to be obtained to solve the equations, see Fig. 4 a). This is of course not an issue in simulation but when tested on a test bench this becomes important. To counter this concern, some simplifications are proposed to reduce the number of variables.

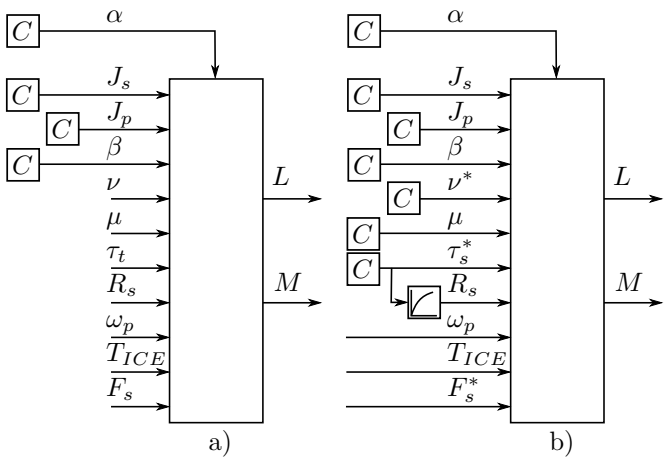


Fig. 4. a) Overview on the inputs to calculate $L$ and $M$. b) Overview on the strictly necessary inputs to calculate $L$ and $M$. The value $C$ stands for a constant.

As constant slip is expected due to proper control, the friction coefficient $\mu$ will be fairly stable. The first adaptation is thus to consider a fixed friction coefficient $\mu$. Furthermore, on the hypothesis of proper slip control, the slip is presumed equal to the setpoint. Based on the assumption of proper slip control and low values for slip it is also possible to equalize the theoretical and the actual speed ratio (see eq. (2)). Combined with an appropriate ratio controller it is possible to obtain $\tau_t$ and the running radii $R_{p,s}$ directly from the speed ratio setpoint. The last simplification is to use the output of the slip controller to estimate the force on the secondary pulley $F_s$ instead of measuring the clamping force.

Due to these changes, only 2 measurements remain: speed of the primary pulley $\omega_p$ and the torque on the primary pulley $T_{ICE}$. Of these variables speed is easily measured and torque of the ICE could be estimated based on engine characteristics (Zweiri et al. (2006)) to avoid an expensive torque sensor.

## 5. RESULTS

### 5.1 Impact of the parameter $\alpha$

As mentioned in section 4.3, the proportional gain $K_p$ was defined with one degree of freedom left. This allows the control engineer to test the behavior of the controlled system on torque disturbances. Fig. 5 shows the response for varying $\alpha$ values. At t equal to 2.5s there is a stepwise load variation of 25Nm which is in correspondence with the test done by Bonsen et al. (2005a). In all cases, the controller is able to stabilize the slip, however the larger the value for $\alpha$, the more immune the controlled system becomes for the specific load variation. Furthermore it is possible to conclude that there is no further improvement of the response of the controller for $\alpha$ values larger than 250. Therefore, the remaining simulations have been performed with $\alpha$ equal to 250.

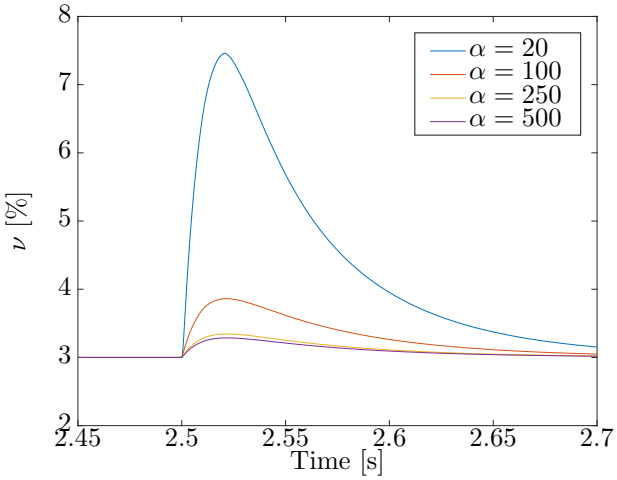


Fig. 5. Slip variation due to a stepwise load variation of 25Nm at t=2.5s for varying values of $\alpha$.

### 5.2 Varying load at constant speed ratio

In the previous subsection, the impact of one specific load disturbance is highlighted to analyze the impact of the factor $\alpha$. In this subsection the results are discussed of both positive and negative load disturbances of varying magnitude. Fig. 6 shows that the magnitude of the load variation has no significant impact on the settling time of the controller. Only the overshoot increases for increasing load. Fig. 6 also shows that not only the force on the secondary pulley changes due to the load variations but also the force on the primary pulley. The reason for this effect is that the speed ratio of the CVT is defined by the ratio of both forces on the pulleys as already mentioned in subsection 4.2. As the secondary force needs to be changed to maintain a constant value for the slip, the primary force needs to change as well to maintain the desired, constant, value for the speed ratio.

### 5.3 Varying speed ratio at constant load

According to eq. (10), the speed ratio could also be a disturbance for the slip controller. However, Fig. 7 shows that the proposed control architecture has no difficulties with sustaining constant slip values while the speed ratio is following a desired curve. Note that there are 2 peaks in the profile of the secondary clamping force. By increasing the force on the secondary clamping force the torque $T_s$ developed by that pulley increases. As a result the secondary pulley is accelerated by which the imposed speed ratio $\tau_s^*$ value is maintained.

### 5.4 Varying speed ratio and load

Fig 6 and 7 clearly showed the interaction between the slip and ratio controller but in those cases speed ratio or load

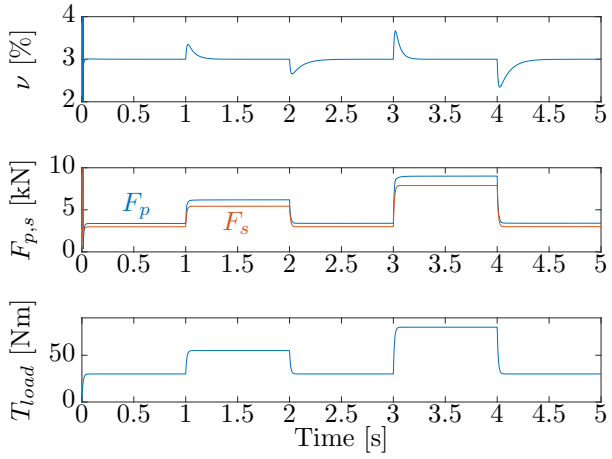


Fig. 6. Slip $\nu$ and clamping forces $F_{p,s}$ for load torque $T_{load}$ variations in function of time at constant speed ratio $\tau_s$ of 1.

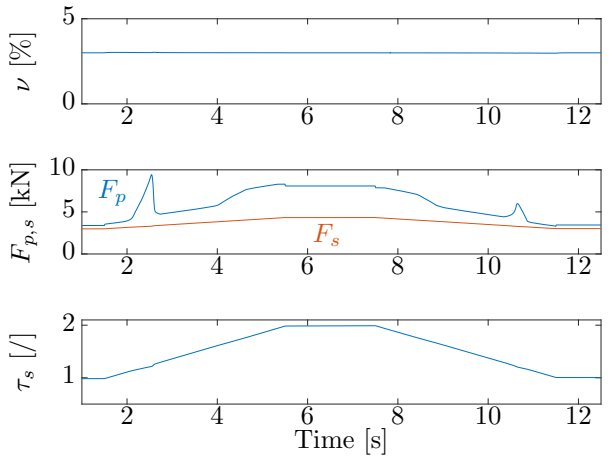


Fig. 7. Slip $\nu$, clamping forces $F_{p,s}$ and speed ratio $\tau_s$ in function of time for a constant load torque $T_{load}$ of 30Nm.

torque were constant. Fig. 8 shows that the controllers can also handle simultaneous variations of load torque and speed ratio. As in Fig. 6, a small increase in slip is noticeable due to the increased load torque. The impact due to ratio variation is non-existent.

Fig. 9 shows the corresponding clamping forces which show to be in coherence with the previously presented data. Again due to ratio variation, a peak in the clamping force profile of the primary pulley appears in order to increase the torque on that pulley. After 3s the clamping forces increase due to varying load torque similar to the results shown in Fig. 6.

Besides the corresponding clamping forces, it is also useful to plot $K_p$ and $T_i$ for this simulation. Fig. 10 shows that, for this case, $K_p$ starts varying when the speed ratio changes. Moreover, the impact of the stepwise load torque variation is not visible in the value for $K_p$. This makes sense as $K_p$ is only a function of $\alpha$ and $L$ (see eq. (21)) which do not depend on the load torque $T_{load}$. This is in contrast with the integral term $T_i$ where a steep decrease is noticeable after 3s. Furthermore $T_i$ also varies during ratio variation. This can also be clarified as $T_i$ depends uniquely on $M$ (see eq. (18)) which is a function of, among others, torque and speed ratio. Fig. 10 thus clearly demonstrates the dependency of the controller settings on the operating conditions.

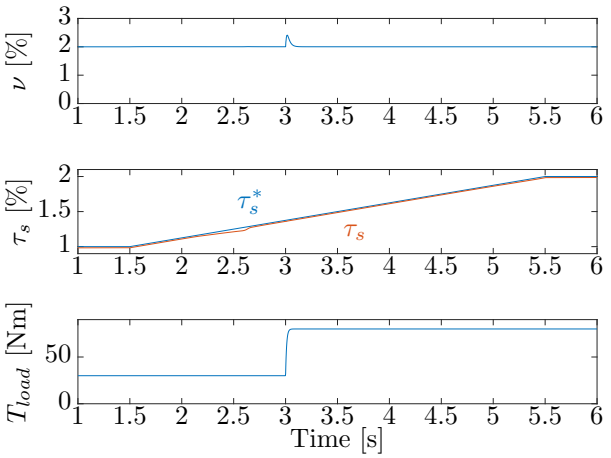


Fig. 8. Slip $\nu$, speed ratio $\tau_s$ and load torque $T_{load}$ in function of time.

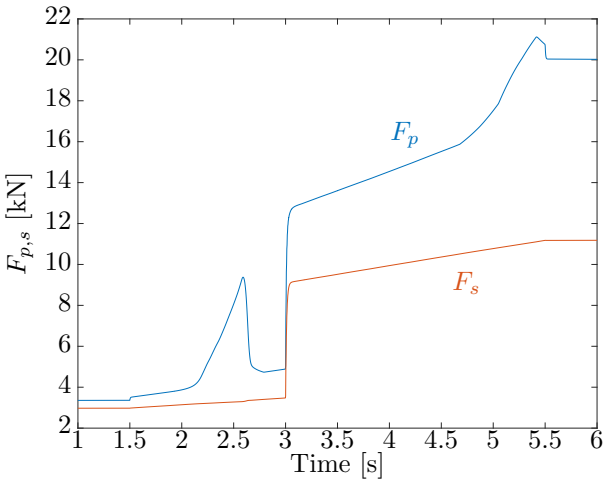


Fig. 9. Corresponding clamping forces $F_{p,s}$ for Fig. 8 in function of time.

## 6. CONCLUSION

In this paper a method is elaborated to design a PI controller for a slip controlled belt CVT. In contrast to earlier literature, this paper proposes a straightforward adaptive controller without losing robustness. To this end the complex nonlinear slip dynamics were simplified to a first order transfer function which enabled the use of basic control design rules. The results which were obtained based on a detailed model, show that the slip controller can handle torque disturbances and is immune for speed ratio variations. These results justify the simplifications which were made in the controller design. Based on these promising results, measurements on a test bench can be done to see wheter these simplifications still hold.

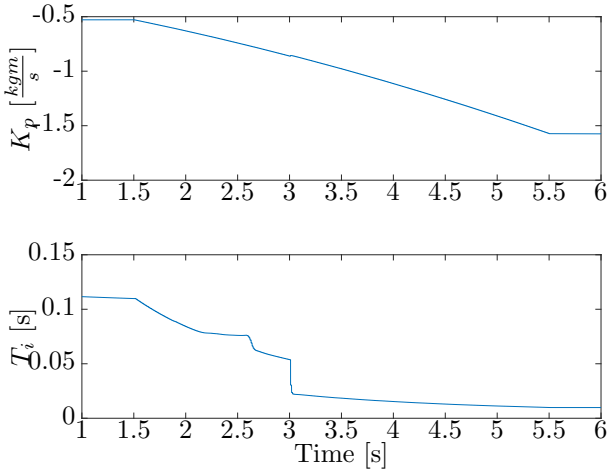


Fig. 10. Corresponding controller parameters $K_p$ and $T_i$ for Fig. 8 in function of time.

## ACKNOWLEDGEMENTS

This research is carried out for the EMTechno project (project ID: IWT150513) supported by VLAIO and Flanders Make, the strategic research center for the manufacturing industry.

## REFERENCES

Akehurst, S., Parker, D.A., and Schaaf, S. (2007). Dynamic modeling of the Milner continuously variable transmission - The basic kinematics. *Journal of Mechanical Design*, 129(11), 1170–1178.

Bonsen, B., Klaassen, T., Pulles, R., Simons, S., Steinbuch, M., and Veenhuizen, P. (2005a). Performance optimisation of the push-belt CVT by variator slip control. *International Journal of Vehicle Design*, 39(3), 232. doi: 10.1504/IJVD.2005.008473.

Bonsen, B., Pulles, R.J., Simons, S.W.H., Steinbuch, M., and Veenhuizen, P.A. (2005b). Implementation of a slip controlled CVT in a production vehicle. In *Control Applications, 2005. CCA 2005. Proceedings of 2005 IEEE Conference on*, 1212–1217.

Carbone, G., Mangialardi, L., Bonsen, B., Tursi, C., and Veenhuizen, P.A. (2007). CVT dynamics: Theory and experiments. *Mechanism and Machine Theory*, 42(4), 409–428.

Carbone, G., Mangialardi, L., and Mantriota, G. (2001). Fuel Consumption of a Mid Class Vehicle with Infinitely Variable Transmission. In *SAE Technical Papers*, 2474–2484.

Carbone, G., Mangialardi, L., and Mantriota, G. (2004). A comparison of the performances of full and half toroidal traction drives. *Mechanism and Machine Theory*, 39(9), 921–942.

Chen, X., Hang, P., Wang, W., and Li, Y. (2017). Design and analysis of a novel wheel type continuously variable transmission. *Mechanism and Machine Theory*, 107(4800), 13–26.

Kempermann, C. (2007). Hydrostatic variators for stepless transmissions - Aspects of CVT technology from a supplier's viewpoint. In *VDI-Berichte*, 121–126.

Panagopoulos, H., Åström, K.J., and Hagglund, T. (2002). Design of PID controllers based on constrained optimisation. *IEE Proceedings - Control Theory and Applications*, 149(1), 32.

Simons, S., Klaassen, T., Veenhuizen, P., and Carbone, G. (2008). Shift dynamics modelling for optimisation of variator slip control in a pushbelt CVT. *International Journal of Vehicle Design*, 48(1/2), 45.

Srivastava, N. and Haque, I. (2009). A review on belt and chain continuously variable transmissions (CVT): Dynamics and control. *Mechanism and Machine Theory*, 44(1), 19–41.

Van der Sluis, F., Van Dongen, T., Van Spijk, G.J., Van der Velde, A., and Van Heeswijk, A. (2006). Fuel consumption potential of the pushbelt CVT. In *Proceedings of FISITA 2006 World Automotive Congress*, 1–12.

Zweiri, Y.H., Whidborne, J.F., and Seneviratne, L.D. (2006). Diesel Engine Indicated and Load Torque Estimation Using Sliding Mode Observer. *Journal of Automobile Engineering*, 220(6), 95–103.